Progress In Electromagnetics Research B, Vol. 11, 155–172, 2009

MIXED ECCENTRICITY FAULT DIAGNOSIS IN SALIENT-POLE SYNCHRONOUS GENERATOR USING MODIFIED WINDING FUNCTION METHOD

J. Faiz, B. M. Ebrahimi, and M. Valavi

Department of Electrical and Computer Engineering
University of Tehran
Tehran, Iran

H. A. Toliyat

Department of Electrical Engineering
Texas A & M University
College Station, TX 77843, USA

Abstract—In this paper, winding function method (WFM), applied to a faulted synchronous generator, is modified and is used for on-line diagnosis of mixed eccentricity fault. For the first time, the static and mixed eccentricities are modeled in synchronous generators. A modified winding function (MWF) method introduced here is more precise compared with previous methods. This MWF enables to compute the air gap magnetic permeance accurately. Here, two or three terms of the infinity permeance series have not been used, but a closed form equation is employed for permeance evaluation. This leads to a very precise computation of the inductances of the faulted machine. Self inductances of the stator and rotor, mutual inductance of two stator phases and the mutual inductance of rotor and stator are obtained. Meanwhile, it is shown that static, dynamic and mixed eccentricities lead to the increase of the amplitude and occurrence of the distortion in the aforementioned inductances. Since calculation of inductances is the most important step for fault diagnosis of the machine, the proposed method improves the on-line diagnosis of the fault. Meanwhile, the spectrum analysis of stator current, obtained from experimental results, is illustrated.

1. INTRODUCTION

Consequence of many electrical and mechanical faults occurring during the operation of electrical machines is the eccentricity between the rotor and stator. They are categorized into three general groups: static eccentricity (SE), dynamic eccentricity (DE) and mixed eccentricity (ME). In static eccentricity (Fig. 1(a)) the symmetrical axis of rotor coincides with rotor rotating axis, while stator symmetrical axis is displaced with respect to aforementioned axis. In this case, air gap distribution is non-uniform but the minimum air gap angular position is fixed. In dynamic eccentricity (Fig. 1(b)), only the rotor symmetrical axis is displaced with respect to rotor rotation axis, which coincides with stator symmetrical axis. Fig. 1 shows the cross section of the healthy and faulty salient pole synchronous generator under static eccentricity. In mixed eccentricity condition, both symmetrical and rotor rotation axes are displaced with respect to the stator rotation axis. Indeed, in the mixed eccentricity each of three stator, rotor and rotational symmetrical axes is displaced with respect to the others. Fault diagnosis systems are employed as a tool to maintain and protect the costly systems against fault. These systems receive the necessary information from the system or process and determine its performance. If this agrees with the predefined faults conditions, the relevant fault is announced. The most important profit of the fault diagnosis system is that the probable fault of the system can be predicted by on-line analysis of the system parameters and be prevented from extension [1–4]. Inductances of the salient pole synchronous generator are calculated under dynamic eccentricity, using FEM and considering both magnetic saturation and geometrical specifications of the machine in [6]. Then, by means of Discrete Fourier Transform (DFT), the

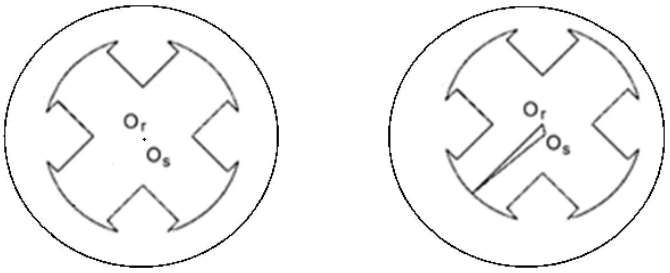

Figure 1. Position of rotor and stator air-gap, (a) healthy and (b) with static eccentricity.

distribution of magnetic fields and the inductances of machine are gone under harmonic analysis. In [7], the static and dynamic eccentricities are diagnosed using inductive sensors mounted on the stator chamber and the processing is done on the modulation functions obtained from induced voltage in sensor loops. The mentioned processing is applied on envelop of the harmonic variations curve. The generator under fault is modeled using FEM in [8]; turning current in the parallel windings of the stator is studied for abnormal functioning like internal short circuit and eccentricity and the harmonics of these turning currents are investigated. In [9], using the theory of modified winding function method (MWFM), the modeling and simulation of salient pole synchronous generator is done under dynamic eccentricity. Then the inductances of machine are calculated and the stator current is obtained using electromagnetic coupling equations. Also, by means of fast Fourier transform (FFT), the spectrum of this signal is used to diagnose the dynamic eccentricity and the index of fault diagnosis is introduced to be the amplitude of harmonics of stator current, especially for harmonics 17 and 19. In [10], a synchronous machine under internal faults has been modeled based on the actual winding arrangement. Then, using winding function approach, the machine inductances have been calculated directly from the machine winding distribution, thereby the space harmonics produced by the machine windings have been readily taken into account. In [11], a new linear model of a salient pole three phase synchronous machine under eccentricity faults condition is presented based on WFM considering the geometry and the physical layout of all windings. In [12], the FEM is implemented on a salient pole synchronous machine with help of the Maxwell 2D Field Simulator package. Flux distribution, self and mutual inductance of machine in case of healthy and dynamic eccentric rotor are calculated from FEM. It is shown that ignoring the nonlinearity in magnetic material in FE analysis causes the results of FEA and WFM to be in close agreement. In [13], two air gap search coil method applied to detect static and dynamic eccentricity fault in synchronous machine. It is shown that the odd multiples harmonic of fundamental frequency present at EMF of search coils in the presence of static eccentricity fault. Also, the sum of each pair of harmonics amplitude produced by dynamic eccentricity is approximately equal to the corresponding intermediate static eccentricity. The stator current and shaft signal of synchronous machine are essential two parameters which have been studied for analysis of this machine under eccentricity faults. In [14, 15], effects of eccentricity fault have been studied on shaft signals of synchronous machine. These studies show that the shaft signals reduce in tilted rotor condition due to opposite shaft flux linkage

at both ends. Also, the amplitude of shaft signal is in proportion with the eccentricities. In [16], using analytical method and FEM saturation effects on unbalanced magnetic pull (UMP) in no-load and full-load synchronous machine under 20% eccentricity have been investigated. It is shown that considering of saturation is necessary to compute UMP in faulty synchronous machine precisely. Although the WFM has been widely utilized for faulty synchronous generators analysis, in [9, 11], symmetrical air gap is considered. Revising the assumptions and fundamental equations of this theory showed that the winding function for non-uniform air gap differs from that of the uniform air gap and this modified winding function method (MWFM) has been recently used for the analysis and fault diagnosis of a synchronous generator [17]. In this paper, the MWFM is modified to evaluate inductances of the faulty synchronous generator precisely which can be used for on-line diagnosis of mixed eccentricity fault. A MWFM introduced here enables to compute the air gap magnetic permeance more accurately. Here, two or three terms of the infinity permeance series has not been used, but a closed form equation is employed for a very precise evaluation of the inductances of the faulted machine. Then, for the first time, the static and mixed eccentricities are modeled in synchronous generators to investigate the faulty synchronous generator performance comprehensively.

In this paper, in Section 2 the synchronous generator under static, dynamic and mixed fault is modeled and analyzed using MWFM. In Section 3, the self inductance of stator and mutual inductance of the two phases of the stator are calculated for generator under static and dynamic eccentricities. In Section 4, the self inductance of rotor and mutual inductance of rotor and stator is calculated for generator under static and dynamic eccentricities. In Section 5, the self inductance of stator and mutual inductance of the two phases of the stator are calculated for generator under mixed eccentricities. In Section 6, the experimental results for the frequency spectrum stator current of the generator under dynamic eccentricity is calculated. Table 1 summarizes the specifications of the proposed generator.

2. A MODIFIED WINDING FUNCTION THEORY

Considering field components is necessary in precise modeling of any electrical system [18–22]. Albeit, modeling attitudes such as finite element methods compute variations punctually, requiring a lot of input information. Analytical methods which are utilized in simulating electrical systems, could satisfactorily evaluate variations [23, 24].

The principal equation of the theory which presents the mutual

Table 1. Salient pole synchronous motor parameters used in the simulation.

Generator Power	475 KW
No. of phases	3
Frequency	60 Hz
Power Factor	0.8
Field Voltage	60 V
L	273.05 mm
R	422.656 mm
g	2.54 mm
N_r	108 turns/pole
N_s	3 turns/coil
R_s	0.01592 Ω
R_r	0.3632 Ω

inductance of two arbitrary windings x and y in respect to the winding distribution is as follows [7]:

$$L_{yx} = 2\pi \langle n_x \; n_y \rangle - 2\pi \frac{\langle P n_x \rangle \langle P n_x \rangle}{\langle P \rangle} \tag{1}$$

where operator is defined as the mean of function f over $[0, 2\pi]$ and P is the permeance distribution of the air-gap. If it is an arbitrary angle in the stator reference frame, it follows that:

$$\langle f \rangle = \frac{1}{2\pi} \int_0^{2\pi} f(\alpha)\, d\alpha \tag{2}$$

The derivation of the equations (1) and (2) is discussed in [17]. These equations have been developed by taking into account a more precise distribution of stator phases and rotor excitation windings and also a more precise computation of the air-gap permeance. Its application results are compared with those obtained by the winding function and FE method [9]. This comparison shows that the obtained result is closer to that of the FE computation than that of the normal winding function. Precise fault diagnosis in the salient-pole synchronous generators considering the non-uniform air-gap of the machine is necessary. The distribution of the air-gap of the machine

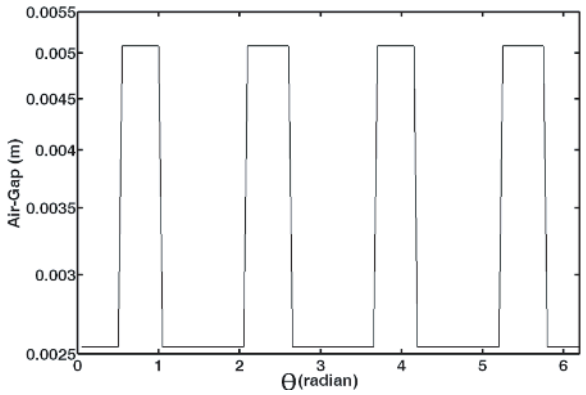

Figure 2. The distribution of the air-gap of the proposed synchronous generator machine.

has been depicted in Fig. 2. Air-gap permeance is proportional to the inverse of the air-gap length. Considering Figs. 1 and 2, this quantity can be neglected for the points far from the poles shoes air- gap, and are taken into account only for the air-gap between the salient-poles and the stator. Therefore, the air-gap permeance distribution, between the salient pole of the rotor and stator, is as follows:

$$P(\alpha) = \mu_0 \frac{r_{av}(\alpha)}{g(\alpha)} \tag{3}$$

where $r_{av}(\alpha)$ and $g(\alpha)$ are the mean radius of air-gap and air-gap distribution, respectively. These two quantities are constant for all the points between the salient-pole and stator, in the symmetrical case. These two geometrical quantities of the machine are calculated in the static and dynamic air-gap eccentricity presented in Fig. 1. It is noted that O_s and O_r are the centerline of rotor and stator respectively. Vector O_sO_r is called the dynamic eccentricity vector and its absolute value is shown by δ. The eccentricity factor is the ratio of the length of this vector, to the symmetrical air-gap length over the pole shoes (g_0). This vector rotates around stator symmetrical axes with angular speed equal to the mechanical speed of the rotor. Therefore, once the motor starts up, it is assumed that this vector coincides with the reference axes of the mechanical angle, and moreover, is always equal to the mechanical angle of the rotor. Fig. 2 shows the position of an arbitrary point M on the rotor pole shoes in the mixed eccentricity condition. The distance of this point from the rotor center is equal to

(rotor radius), then:

$$O_sM = \delta g \cos(\alpha - \theta) + \sqrt{R_r^2 - \delta^2 g^2 \sin^2(\alpha - \theta)} \quad (4)$$

For the inner radius of stator, the mean length and radius of the air-gap above the poles shoes are as follows:

$$g_e(\alpha) = R_s - O_sM \quad (5)$$

$$r_{av}(\alpha) = \frac{1}{2}(R_s - O_sM) \quad (6)$$

Since the air-gap length above the poles shoes is much smaller than the rotor radius, the second term in (4) may be approximated with R_r. Equations (5) and (6) can therefore be rewritten as

$$g_e(\alpha) = g(1 - \delta\cos(\alpha - \theta)) \quad (7)$$

$$r_{av} = r_0 + 0.5\delta g\cos(\alpha - \theta) \quad (8)$$

where the term $0.5 \times \delta g\cos(\alpha - \theta)$ has been ignored due to the small air-gap length compared to the rotor radius. The mean radius of the air-gap poles is therefore almost equal to this radius in the healthy machine. Moreover, the magnetic permeance distribution of the air-gap above the pole shoes is obtained by substituting (7), (8) into (3) as follows:

$$P(\varphi) = \frac{\mu_0 r_0}{g_0(1 - \delta\cos(\alpha - \theta))} \quad (9)$$

Figure 3 presents the polar distribution of air-gap magnetic permeance of a synchronous machine in the healthy condition 25% SE and 25% DE. In such eccentricity, these distributions rotate with mechanical speed of the rotor. In [6], this distribution has been approximated by the first ten terms of its Fourier series, leading to a reduction in the accuracy of the computations.

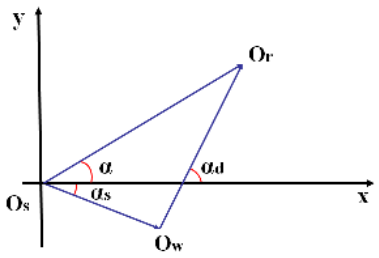

Figure 3. Positions of rotor rotational axis, rotor symmetrical axis and stator symmetrical axis for a mixed eccentricity condition.

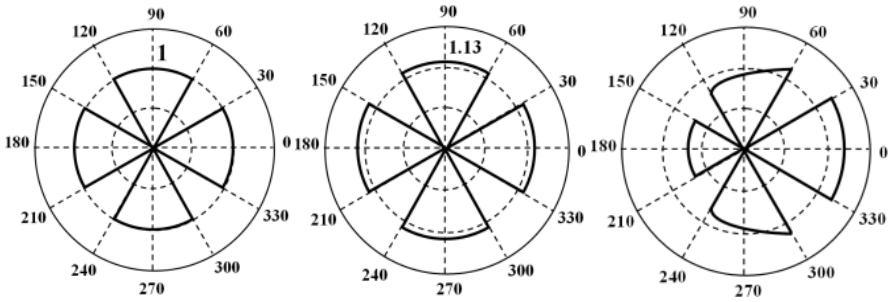

Figure 4. Polar distribution of air-gap permeance of a synchronous machine, (a) Healthy, (b) under static eccentricity and (c) under dynamic eccentricity.

3. COMPUTATION OF STATOR INDUCTANCE FOR SYNCHRONOUS GENERATOR UNDER SE AND DE

3.1. Self-Inductances

Fig. 5 shows the per phase self-inductance of the stator winding of a synchronous generator in healthy, 10%, 20%, 30%, 40% and 50% static and dynamic eccentricities. Comparison of the inductances in Fig. 5 indicates that the static eccentricity increases the above-mentioned inductances as such that the self-inductance of the healthy, 0.173 H increases to 0.198 H in the 50% static eccentricity. Comparison of Fig. 5 and Fig. 6 indicates that the rate of increase of the mutual inductance in static eccentricity is higher than that of the self-inductance. Referring to Fig. 6 it is seen that in addition to the increase of the inductance due to the dynamic eccentricity, there is asymmetrical distribution of the inductance. Comparison of Figs. 5 and 6 shows that the asymmetry occurred in the mutual inductance is higher than that of the self-inductance.

3.2. Mutual Inductances

Fig. 6 shows the mutual-inductance of the first and second phase of the stator winding of a synchronous generator in healthy, 10%, 20%, 30%, 40% and 50% static and dynamic eccentricities. Comparison of the inductances in Fig. 6 indicates that the static eccentricity increases the above-mentioned inductances as such that the self-inductance of the healthy, 0.173 H increases to 0.198 H in the 50% static eccentricity. There is no asymmetry in the inductance distribution. Comparison

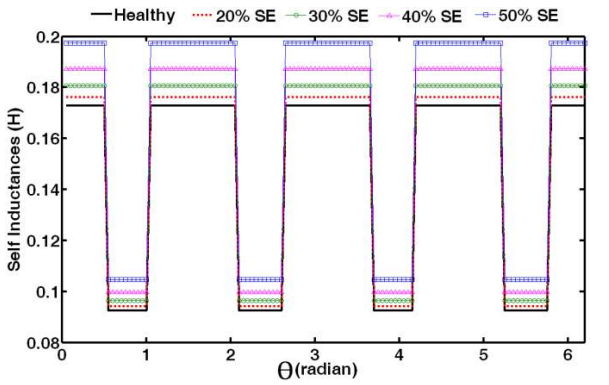

(a)

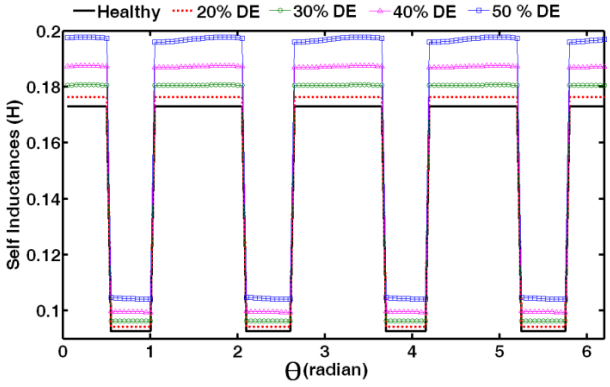

(b)

Figure 5. Per phase self-inductance of the stator winding in healthy, 20%, 30%, 40% and 50%, (a) static eccentricity and (b) dynamic eccentricity.

of these two cases with the case of 50% dynamic eccentricity indicates that the dynamic eccentricity also increases the inductance and creates asymmetrical inductance distribution. The reason is that in the dynamic eccentricity case, the air gap permeance depends on the rotor angular position. Since this angle varies continuously the distribution of the inductance is asymmetrical.

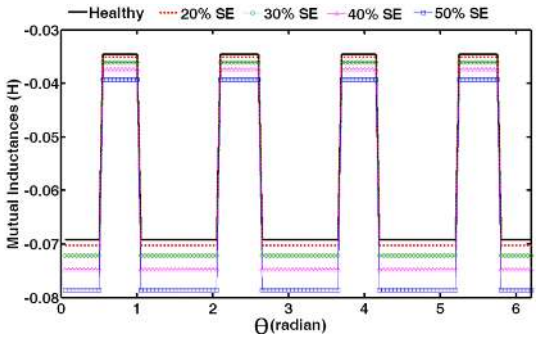

(a)

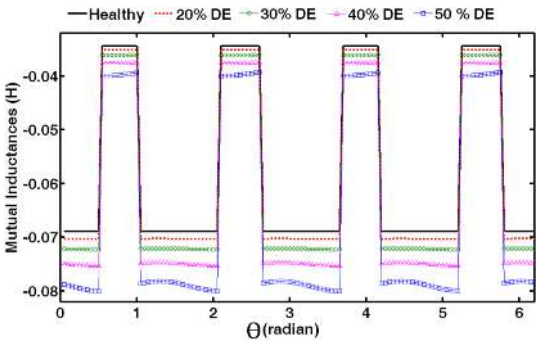

(b)

Figure 6. (Mutual-inductance of the stator winding in healthy, 20%, 30%, 40% and 50%, (a) static eccentricity and (b) dynamic eccentricity.

4. COMPUTATION OF ROTOR INDUCTANCE FOR SYNCHRONOUS GENERATOR UNDER SE AND DE

Fig. 7 shows the per phase mutual-inductance of the stator and rotor windings of a synchronous generator in healthy, 10%, 20%, 30%, 40% and 50% static and dynamic eccentricities. Fig. 7 indicates that the static eccentricity increases the mutual inductance of the healthy machine, 1.45 H to 1.68 H in the faulty case. Comparison of Figs. 7(a) and 7(b) indicates that the rate of increase in the rotor mutual inductance in dynamic eccentricity case is larger than the static eccentricity case. Also dynamic eccentricity increases the inductance and asymmetrical degree in the mutual-inductance distribution (Fig. 7b). Comparison of Figs. 4(b) and 5(b) indicates that the rate of the rotor mutual-inductance increase is higher than the stator inductance in the dynamic eccentricity case.

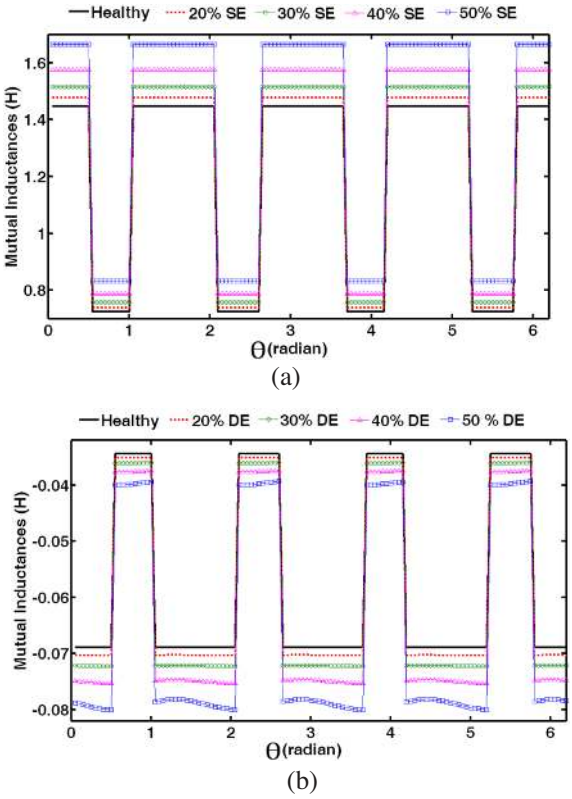

Figure 7. Mutual-inductance of the stator and rotor windings in healthy, 20%, 30%, 40% and 50%, (a) static eccentricity and (b) dynamic eccentricity.

5. COMPUTATION OF STATOR INDUCTANCE FOR SYNCHRONOUS GENERATOR UNDER ME

5.1. Self-Inductances

Fig. 8(a) shows the self-inductance of the first phase of the stator winding of a synchronous generator in healthy and mixed eccentricity (20% SE and 30% DE) cases. Comparison of the inductances indicates that the mixed eccentricity increases the above-mentioned inductances and also leads to asymmetrical distribution of the stator windings inductances. The reason is that in the mixed eccentricity, the air gap permeance depends on the angular position of the rotor; since this angle continuously varies, the inductance distribution of a mixed eccentricity machine is asymmetrical.

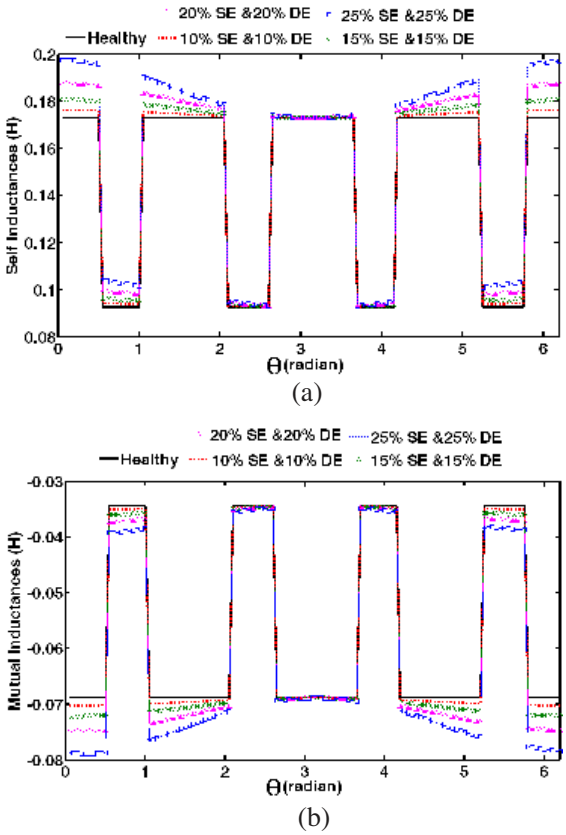

Figure 8. Inductance of healthy and faulty synchronous generator under mixed eccentricity (a) self-inductance and (b) mutual-inductance.

5.2. Mutual Inductances

Fig. 8(b) shows the mutual-inductance of the first and second phase of the stator winding of a synchronous generator in healthy and mixed eccentricity (20% SE and 30% DE) cases. Comparison of the inductances indicates that the mixed eccentricity increases the above-mentioned inductances and also leads to asymmetrical distribution of the stator windings inductances. Comparison of Figs. 8(a) and Fig. 8(b) indicate that the rate of increase of the self-inductance is lower than that of the mutual inductance of the stator winding. Referring to Fig. 8 demonstrates that rise of eccentricity degrees increases the amplitude and variation rates of machine inductances. Meanwhile, their variation rate has been extended by increase of eccentricity

degree. Increases of amplitude and distortion of machine inductances distorts stator current and rises the amplitude of side-band components in spectral of stator current which can be utilized as an appropriate index for non-invasive eccentricity fault diagnosis.

6. EXPERIMENTAL RESULTS

To study the effect of dynamic eccentricity on synchronous machines, an experiment has been performed on a round-rotor synchronous motor. The motor is a three-phase type, 1 KW, 208 V, 1.7 A, and 1800 r/min. To conduct the experiment, the motor has been loaded separately with two discs of the same size. The first disc has a smooth solid surface to emulate the case of the non-eccentric rotor and the other disc has been drilled with four small holes on one side of it to emulate the case of rotor dynamic eccentricity. To study the effect of dynamic eccentricity on the stator and rotor current signatures, the motor is first loaded with the smooth surface disc, and then the stator current and their frequency harmonics have been captured. Fig. 7 reveals the stator current waveform for the case of the symmetric rotor. Fig. 8 shows the upper harmonics, including the 19th frequency component of the stator current. To impose dynamic eccentricity on the rotor, the first disc coupled to the rotor shaft has been replaced by the second disc that has the drilled holes. Fig. 9 illustrates the

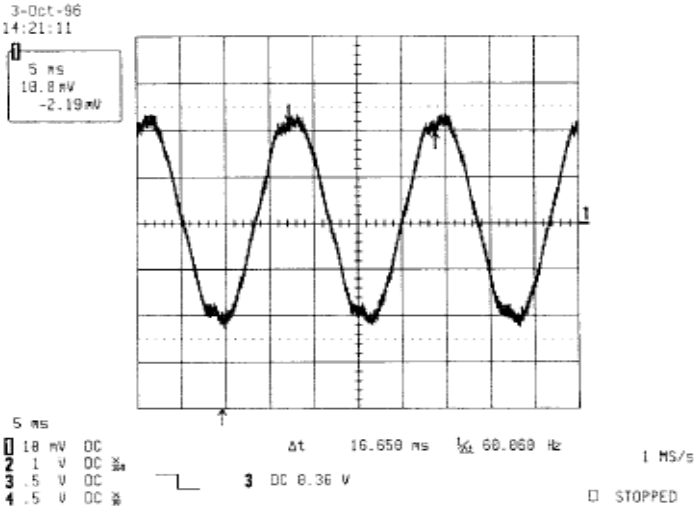

Figure 9. Stator current waveform with symmetric disc, 0.5 A/div.

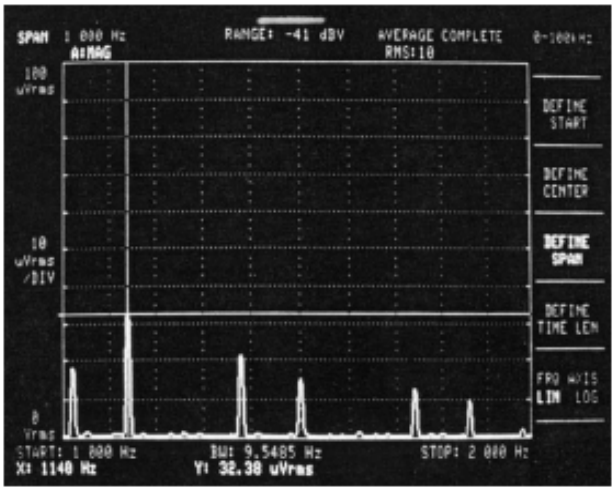

Figure 10. Stator current frequency spectrum of symmetric disc, 1000–2000 Hz.

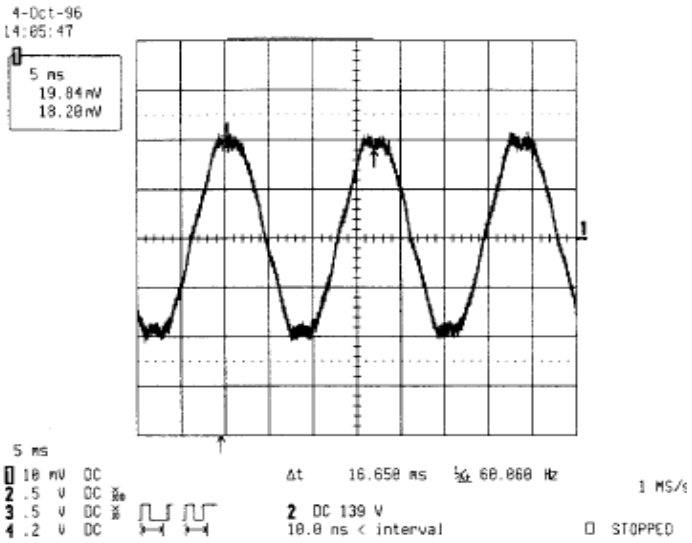

Figure 11. Stator current waveform with nonsynchronous disc, 0.5 A/div.

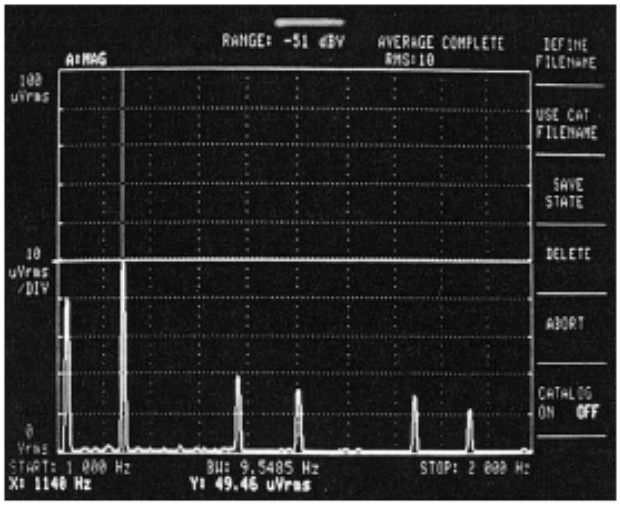

Figure 12. Stator current frequency spectrum of non-symmetric disc, 1000–2000 Hz.

stator current waveforms in the case of the eccentric rotor. It is clear that the 17th and 19th harmonics of Fig. 10 have increased more rapidly due to the dynamic air-gap eccentricity. Table 2 summarizes relative percentage increase of stator current harmonics due to dynamic eccentricity.

Table 2. Relative percentage increase of stator harmonics due to rotor eccentricity.

5th	7th	11th	13th	17th	19th
3.1%	3.2%	0.8%	70.0%	110.5%	52.74%

7. CONCLUSION

In this paper static, dynamic and mixed eccentricities were modeled and analyzed using MWFEM. This modeling method provided us with exact calculation and analysis of air gap permeance and so the machine inductances were calculated precisely. It was shown that, static, dynamic and mixed eccentricities increase the magnitude, distort the distribution and these both affect machine inductances. The stator current spectrum in healthy and under fault generator was

calculated and it was shown that the occurrence of eccentricity causes the amplitude of harmonic components to increase, which can be used as a proper index to recognize eccentricity occurrence and detect its degree.

REFERENCES

1. Faiz, J., B. M. Ebrahimi, B. Akin, and H. A. Toliyat, "Finite element transient analysis of induction motors under mixed eccentricity fault," *IEEE Trans. on Magnetics*, 66–74, Jan. 2008.
2. Faiz, J., B. M. Ebrahimi, B. Akin, and H. A. Toliyat, "Comprehensive eccentricity fault diagnosis in induction motors using finite element," Accepted in *IEEE Trans. on Magnetics*, 2008.
3. Faiz, J. and B. M. Ebrahimi, "Mixed fault diagnosis in three-phase squirrel-cage induction motor using analysis of air-gap magnetic field," *Progress In Electromagnetics Research*, PIER 64, 239–255. 2006.
4. Faiz, J., B. M. Ebrahimi, and M. B. B. Sharifian, "Time stepping finite element analysis of rotor broken bars fault in a three-phase squirrel-cage induction motor," *Progress In Electromagnetics Research*, PIER 68, 53–70, 2007.
5. Faiz, J. and B. M. Ebrahimi, "Static eccentricity fault diagnosis in an accelerating no-load three-phase saturated squirrel-cage induction motor," *Progress In Electromagnetics Research B*, Vol. 10, 35–54, 2008.
6. Zhu, J. and A. Qiu, "Inductance calculation of large salient-pole synchronous generators with air-gap eccentricity," *IEEE Conference on Electromagnetic Field Computation*, 264, 2006.
7. Melgoza, J. J. R., G. T. Heydt, A. Keyhani, B. L. Agrawal, and D. Selin, "An algebraic approach for identifying operating point dependent parameters of synchronous machines using orthogonal series expansions," *IEEE Transaction on Energy Conversion*, Vol. 16, No. 1, 92–98, Mar. 2001.
8. Foggia, A., J. E. Torlay, C. Corenwinder, A. Audoli, and J. Herigault, "Circulation current analysis in the parallel connected winding of synchronous generators under abnormal operating conditions," *Electric Machines and Drives, International Conference IEMD '99*, 634–636, 1999.
9. Toliyat, H. A. and N. A. Al-Nuaim, "Simulation and detection of dynamic air-gap eccentricity in salient-pole synchronous machines," *IEEE Trans. Ind. Applicat.*, Vol. 35, 86–93, Feb. 1999.

10. Tu, X., L. A. Dessaint, M. El Kahel, and A. O. Barry, "A new model of synchronous machines internal faults based on winding distribution," *IEEE Transaction on Industry Electronics*, Vol. 53, No. 6, 1818–1828, Dec. 2006.
11. Al-Nuaim, N. A. and H. A. Toliyat, "A novel method for modeling dynamic air-gap eccentricity in synchronous machines based on modified winding function theory," *IEEE Transaction on Energy Conversion*, Vol. 13, No. 2, 156–162, June 1998.
12. Tabatabaei, I., J. Faiz, H. Lesani, and M. Nabavi, "Modeling and simulation of salient synchronous generators with dynamic eccentricity using modified winding fnction theory," *IEEE Trans. on Magnetics*, Vol. 40, No. 3, 1550–1555, May 2004.
13. Stoll, R. L. and A. Hennache, "Method of detecting and modeling presence of shorted turns in DC field winding of cylindrical rotor synchronous machines using two airgap search coil," *IEE Proceeding*, Vol. 135, No. 6, 281–294, 1988.
14. Hsu, J. S. and J. Stein, "Effect of eccentricities on shaft signals studied through winding less rotors," *IEEE Transaction on Energy Conversion*, Vol. 9, No. 3, 564–571, 1994.
15. Hsu, J. S. and J. Stein, "Shaft signal of salient-pole synchronous machines for eccentricity and shorted-field-coil detections," *IEEE Transaction on Energy Conversion*, Vol. 9, No. 3, 572–578, 1994.
16. Wamkeue, R., I. Kamwa, and M. Chacha, "Line-to-line short circuit based finite-element performance and parameter predictions of large hydro generators," *IEEE Transaction on Energy Conversion*, Vol. 18, No. 3, 370–378, 2003.
17. Faiz, J. and I. Tabatabaei, "Extension of winding function theory for non-uniform air-gap of electric machinery," *IEEE Trans. on Magnetics*, Vol. 38, 3654–3657, Nov. 2002.
18. Nickelson, L., S. Asmontas, R. Martavicius, and V. Engelson, "Singular integral method for the pulse-modulated microwave electric field computations in a 3D heart model," *Progress In Electromagnetics Research*, PIER 86, 217–228, 2008.
19. Hémon, R., P. Pouliguen, H. He, J. Saillard, and J.-F. Damiens, "Computation of EM field scattered by an open-ended cavity and by a cavity under radome using the iterative physical optics," *Progress In Electromagnetics Research*, PIER 80, 77–105, 2008.
20. Song, T.-X., Y.-H. Liu, and J.-M. Xiong, "Computations of electromagnetic fields radiated frp, cp,plex lightning channels," *Progress In Electromagnetics Research*, PIER 73, 93–105, 2007.
21. Hussein, K. F. A., "Efficient near-field computation for radiation

and scattering from conducting surfaces of arbitrary shape," *Progress In Electromagnetics Research*, PIER 69, 267–285, 2007.

22. Lesselier, D. and B. Duchene, "Buried, 2-D penetrable objects illuminated by line sources: FFT-based iterative computations of the anomalous field," *Progress In Electromagnetics Research*, PIER 05, 351–389, 1991.
23. Nesterenko, M. V., V. A. Katarich, Y. M. Penkin, and S. L. Berdnik, "Analytical methods in theory of slot-hole coupling of electrodynamic volumes," *Progress In Electromagnetics Research*, PIER 70, 79–174, 2007.
24. Gaffour, L., "Analytical method for solving the one-dimensional wave equation with moving boundary," *Progress In Electromagnetics Research*, PIER 20, 63–73, 1998.